Indonesian Journal of Science & Technology

Journal homepage: http://ejournal.upi.edu/index.php/ijost/

Step-by-Step Fabrication of PVDF-TiO2 Hollow Fiber Membrane and Its Application Desalination of Wetland Saline Water via Pervaporation

M. Mahmud[1], Muthia Elma[1,], Aulia Rahma[1], Nurul Huda[1], Riani Ayu Lestari[1], Awali S. K. Harivram[1], Erdina L. A. Rampun[1], Mohd H. D. Othman[2], Muhammad Roil Bilad[3]*

[1]Lambung Mangkurat University, Banjarbaru, Indonesia
[2]Advanced Membrane Technology Research Centre, Universiti Teknologi Malaysia, Johor, Malaysia
[3] Department of Chemical and Process Engineering, Universiti Brunei Darussalam, Brunei Darussalam.
Correspondence: E-mail: melma@ulm.ac.id

ABSTRACT

Wetland water is opted as the source of domestic water supply when the availability of clean fresh water is scarce. Wetland water requires proper treatment due to the high concentration of organic matter and high salinity, particularly in the dry season. This research aims to synthesize, characterize, and investigate the performance of polyvinylidene fluoride (PVDF)-TiO_2 hollow fiber membrane for wetland saline water desalination via pervaporation. The PVDF-TiO_2 hollow fiber membranes were fabricated through the dry wet spinning method under various air gaps (10, 15, and 20 cm). Then, the resulting membranes were tested in a pervaporation process at temperatures of 25, 40, and 60°C. Results show that the incorporation of TiO_2 into the PVDF matrix imparted hydrophilicity properties into the resultant membranes. The presence of TiO_2 was confirmed by the TiO_2 stretching vibration at 1640 cm^{-1} (FTIR) and the TiO_2 phase at diffraction peaks at 25.5 and 37°. The membranes exhibited the highest water flux (7.48 $kg/m^2.h$) and salt rejection (> 99.5%) at 40°C. Overall, the developed PVDF-TiO_2 hollow fiber membranes showed encouraging results and demonstrated their effectiveness for the desalination of wetland saline water.

ARTICLE INFO

Article History:
Submitted/Received 20 Jul 2023
First Revised 01 Sep 2023
Accepted 16 Oct 2023
First Available online 18 Oct 2023
Publication Date 01 Dec 2023

Keyword:
Desalination,
Dry wet spinning,
Hollow fiber membrane,
PVDF-TiO_2,
Wetland saline water.

1. INTRODUCTION

South Kalimantan-Indonesia is located in the Southern part of Borneo, with a population of ~4.3 million, dominantly covered by tropical. The wetland water is commonly used for domestic usage in remote coastal areas and households that are yet to receive clean water from the municipal water supply. Fundamentally, direct consumption of wetland water is not advisable because it has poor quality, and frequently it becomes saline during the dry season (Elma, Mustalifah *et al*., 2020; Elma, Riskawati *et al*., 2018; Lestari *et al*., 2020; Rahma, Elma, Mahmud, Irawan *et al*., 2019). Wetland saline water contains high salt concentrations of 0.3-3.2 wt% NaCl, which are almost equal to brackish and seawater salt concentrations (Rahma, Elma, Rampun, *et al*., 2020). Hence, a simple yet versatile treatment is required.

Different types of treatments have been explored for wetland saline water such as pervaporation, ultrafiltration, and coagulation (Elma, Rahma *et al*., 2020; Mahmud *et al*., 2020; Rampun, Elma, Syauqiah *et al*., 2019). These treatments enable to remove natural organic matter (NOM) and salinity (Elma, Bilad *et al*., 2022; Elma, Ghani *et al*., 2022; Elma, Mujiyanti *et al*., 2020; Elma, Pratiwi *et al*., 2022; Elma, Rahma *et al*., 2022; Elma, Rahma *et al*., 2020; Mat Nawi *et al*., 2022; Nawi *et al*., 2020; Rahma, Elma, Aliah, *et al*., 2022; Rahma, Elma, Pratiwi *et al*., 2020; Rahma, Elma, Rampun *et al*., 2020; Satria Anugerah *et al*., 2022). Among these treatments, the pervaporation process provides interesting features of less thermal energy consumption compared to membrane distillation because it only requires vacuum conditions (Rampun, Elma, Rahma, *et al*., 2019). Previous studies employed inorganic membranes based on silica materials and removed up to 60% of NOM from wetland saline water (Elma *et al*., 2023; Maulida *et al*., 2023; Pratiwi *et al*., 2023; Rahma *et al*., 2023; Sari *et al*., 2023). The materials could operate with minimum issues of membrane scaling and fouling (Elma, Mujiyanti *et al*., 2020; Elma, Rampun *et al*., 2020).

Polyvinylidene fluoride (PVDF) is a commercial polymer typically used for the fabrication of ultrafiltration and microfiltration membranes but has been used limitedly for water desalination (Li *et al*., 2017). PVDF polymer is desirable since it provides (1) good chemical resistance, (2) chemical stability; (3) temperature stability; and (4) mechanical strength (Deshmukh & Li, 1998; Shi *et al*., 2013). PVDF has been explored for desalination applications due to its high selectivity to reject salt content (Fan & Peng, 2012). However, its inherent hydrophobic properties may cause fouling when used for the traditional pressure-driven filtration processes.

The application of TiO2 as an additive in polymeric membranes has been reported to enhance the membrane properties, i.e. selectivity, permeability, and physical strength, whilst reducing the membrane fouling propensity (Dzinun *et al*., 2016). TiO2 has been chosen due to its low-cost, non-toxic, and commercially available. It reduces the hydrophobicity and imposes anti-fouling properties on the resultant membranes (Parvizian *et al*., 2020; Sun *et al*., 2020). However, those resultant membrane properties were found to be dependent on the membrane's fabrication method. For instance, PVDF-TiO2 hollow fiber membranes fabricated using a wet-spinning method had a strong interaction between polymeric and inorganic networks due to the uniform dispersion of TiO2 within the polymeric matrix. The incorporation of TiO2 into the polymeric matrix increased the average pore size compared to the pristine PVDF membrane (Yu *et al*., 2009).

The dry-wet spinning method is known in membrane fabrication because it has specific benefits such as simplicity, shortening time, and producing asymmetric cross-section structures. In addition, the effect of air gap in

DOI: https://doi.org/10.17509/ijost.v8i3.63433
p- ISSN 2528-1410 e- ISSN 2527-8045

the dry-wet spinning method has been reported in previous studies. The morphological analysis of PVDF membranes prepared under various air gaps (10, 20, 30 cm) was investigated, that the air gap affected the resulting membrane properties such as finger-like structure, membrane roughness, pore size distribution, porosity, hydrophobicity, and tensile strength. Khulbe *et al*. (2007) applied different air gaps from 10 to 90 cm and found their effect on the membrane roughness. They found different roughness between the inner and outer surfaces of the hollow fiber membrane. The air gap significantly affected the water flux membrane as well. The water flux increased at higher air gaps, leading to an increase in membrane pore size.

Li *et al*. (2017) investigated the performance of the PVA/PVDF membrane in the pervaporation desalination process at different operating temperatures (50-90°C) and feed salinities (0-250 g/L NaCl). The water flux was at 8.6 L/m2h for 100 g/L NaCl at 80°C. The loss of water flux occurred when treating a high solute concentration of 250 g/L NaCl. The decline in water flux was mainly attributed to the concentration polarization during the pervaporation process. Such findings concluded that the feed temperature and salinity concentration were crucial parameters in evaluating the pervaporation performance. In other work, a composite hollow fiber membrane was synthesized by blending PVA and nano-TiO2. Interestingly, the membrane could not reject NaCl and Na2SO4 (inorganic salt) in the feed solution because of the Donnan effect between the hydroxyl group on the composite membrane surface with similar ionic states (Li *et al*., 2014).

To our knowledge, the desalination of wetland saline water using PVDF/TiO2 hollow fiber membranes through pervaporation has not yet been reported. This study aims to synthesize, characterize, and investigate the performance of PVDF-TiO2 hollow fiber membranes for wetland saline water desalination via pervaporation. The membranes were synthesized using the dry-wet spinning method at various air gaps (10, 15, 20 cm) to modulate the resultant membrane properties.

2. METHODS

2.1. Chemicals and Materials

Wetland saline water was taken from Muara Halayung village, Banjar District, South Kalimantan-Indonesia in August 2020 during the dry season. PVDF (Kynar 760 powder series) was selected as the base polymer, TiO_2 (Merck) as the additive, Dimethylacetamide (DMAc, QReC) and ethanol as the solvent, demineralize water as the non-solvent, while epoxy resin (E30CL, Loctite Corporation, USA) as the module potting agent. All chemicals, otherwise clearly specified, were used as analytical grade reagents.

2.2. Step-By-Step Method for Membrane Synthesis and Characterization

The synthesis of PVDF-TiO_2 hollow fiber membranes was done according to our earlier works (Kamaludin *et al*., 2019), as detailed in the step-by-step method as follows. PVDF polymer and TiO_2 were dried in an oven at 50°C for 24 h to remove the moisture. Approximately 21 g of PVDF polymer was added into 152 mL of DMAc solution. The mixture was stirred at 530 rpm at 70^{o}C until homogeneous. Then, 6 g of TiO_2 powder was added to the mixture and continuously stirred for 24 h. The resultant dope solution was then cooled to room temperature and degassed in an ultrasonic water bath for 60 min. Finally, the spinning of hollow fiber was performed by loading the degassed dope solution into the dope reservoir through a syringe pump and extruded by spinneret at an extrusion rate of 26 mL/min. The air gap distances were varied by 10, 15, and 20 cm during the spinning process. The resultant membranes were characterized using Scanning Electron

DOI: https://doi.org/10.17509/ijost.v8i3.63433
p- ISSN 2528-1410 e- ISSN 2527-8045

Microscope (SEM) analysis, contact angle, and Fourier Transform InfraRed (FTIR).

2.3. How to Evaluate the Pervaporation Performance

The performance of the PVDF-TiO_2 hollow fiber membrane was tested in the pervaporation set-up as illustrated in **Figure 1**. The performance was assessed in the forms of permeate flux, salt rejection, and organic matter rejection. The feed solution's temperature was varied between 25˚C (room temperature) to 60˚C at a fixed pervaporation duration of 20 minutes. Permeate conductivity (representing the solute concentration) and the absorbance of UV_{254} (representing the NOM concentration) were measured using a conductivity meter and UV-Vis spectrophotometer, respectively. The membrane performance was determined using the equation below:

$$F = \frac{m}{(A\,\Delta t)} \quad (1)$$

$$R = \frac{(Cf - Cp)}{(Cf)} \times 100\% \quad (2)$$

Where F is permeate flux (kg/m^2.h), m is the mass of permeate (kg) retained in the cold trap, A is the surface-active area (m^2), Δt is the time measurement (h), R is rejection (%), C_f and C_p are the feed and permeate concentration (wt%) of solute or organic matter.

3. RESULTS AND DISCUSSION

3.1. Characteristics of Wetland Saline Water

The wetland saline water naturally formed a cloudy brown color caused by the appearance of NOM, as shown in **Figure 2**. The NOM also represents a soluble and insoluble material that directly affects the water quality (Dayarathne *et al*., 2021). The presence of NOM can be proven by using the UV_{254} analysis. **Table 1** shows the inherent water quality of the wetland saline water used in this study. The pH of wetland saline water was around 6.6, still within the WHO standard limit (6.5-8). However, the conductivity and the TDS parameters were higher than the WHO standard; thus, the wetland saline water required further treatment before could be consumed.

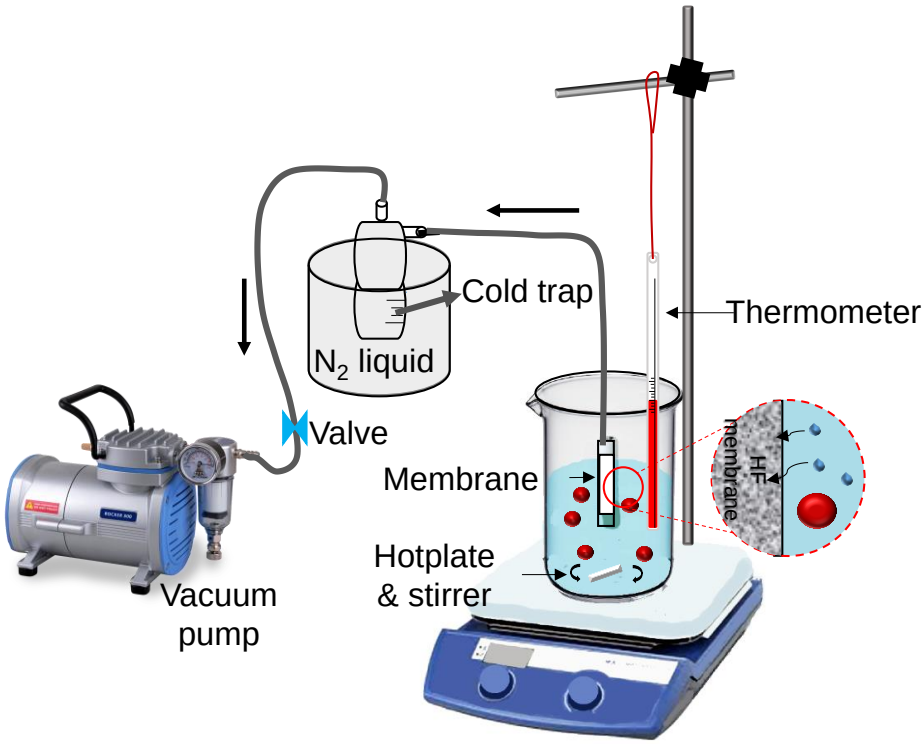

Figure 1. Illustration of pervaporation setup used for evaluating the membrane performance.

DOI: https://doi.org/10.17509/ijost.v8i3.63433
p- ISSN 2528-1410 e- ISSN 2527-8045

Table 1. The inherent water quality of wetland saline water taken in August 2020 at Muara Halayung village (GPS location: -3.479779, 114.621480).

Parameters	Unit	Weeks				Average	Standard
		I	II	III	IV		
pH	-	6.67	6.66	6.64	6.66	6.66	6.5 – 8
Conductivity	ms/cm	9.35	9.34	8.79	8.56	9.01	4 mS/cm
Total Dissolved Solid	mg/L	5400	5370	5365	5360	5373	500
UV_{254}	1/cm	0.315	0.310	0.305	0.295	0.306	-

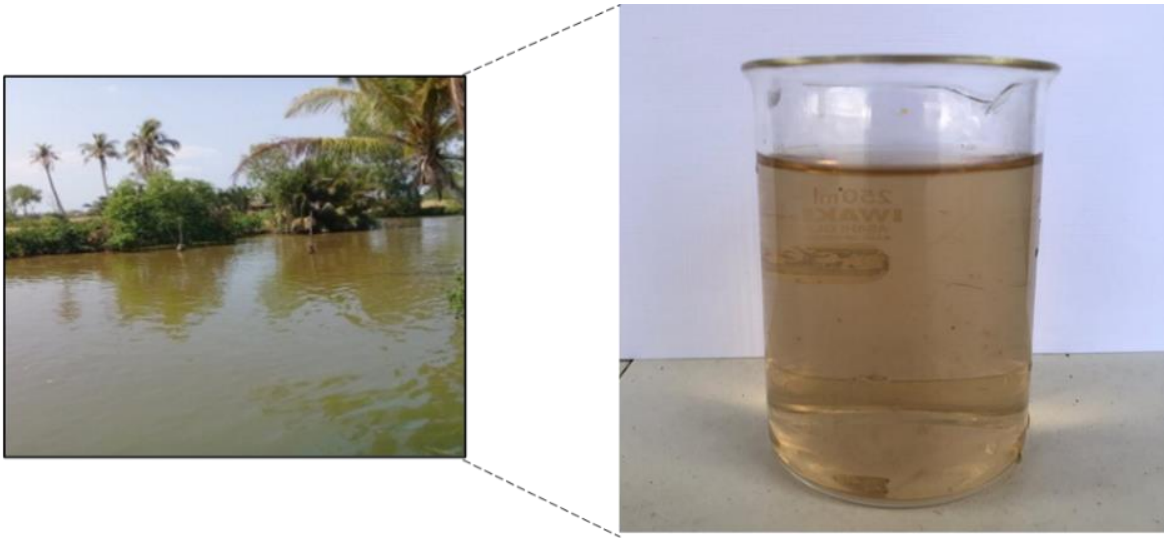

Figure 2. The sampling location (attached photograph picture) and the wetland saline water samples used as the feed for the pervaporation.

3.2. Membrane characteristics

SEM was used as a tool to analyze the surface and cross-section microstructure and morphologies of the resultant PVDF-TiO_2 membranes. Step-by-step analysis of the membrane microstructure based on the obtained SEM images is discussed as follows. Based on **Figure 3 (a-c)**, the cross-section images of the membrane can be observed. It has a macro void that resembles a finger-like structure combined with a sponge-like structure. It is a type of asymmetric pore that is formed by the phase inversion method (Kingsbury & Li, 2009; Wang *et al*., 2016).

The macro void structures were formed close to the inner and outer membrane surfaces. The sponge-like pores consisted of an interconnected network type and a closed-cell type within the entire membrane structure. Such structure formation was attributed to the exchanging process between non-solvent and strong solvents during the phase separation as reported earlier (Tan & Rodrigue, 2019).

The white spots visible in **Figure 3(d)**, proved the presence of TiO2 embedded as part of the membrane matric. The presence of TiO2 reduced the formation of finger-like pores massively, as discussed elsewhere (Kamaludin *et al*., 2019). TiO2 presence increases the viscosity of a dope polymer solution hence altering the path of polymer-solvent-nonsolvent compositions during the phase inversion process. The aggregation of TiO2 particles led to a rougher membrane surface for the PVDF-TiO2 membrane compared to the pristine PVDF membrane, as also found by others (Sakarkar *et al*., 2020).

DOI: https://doi.org/10.17509/ijost.v8i3.63433
p- ISSN 2528-1410 e- ISSN 2527-8045

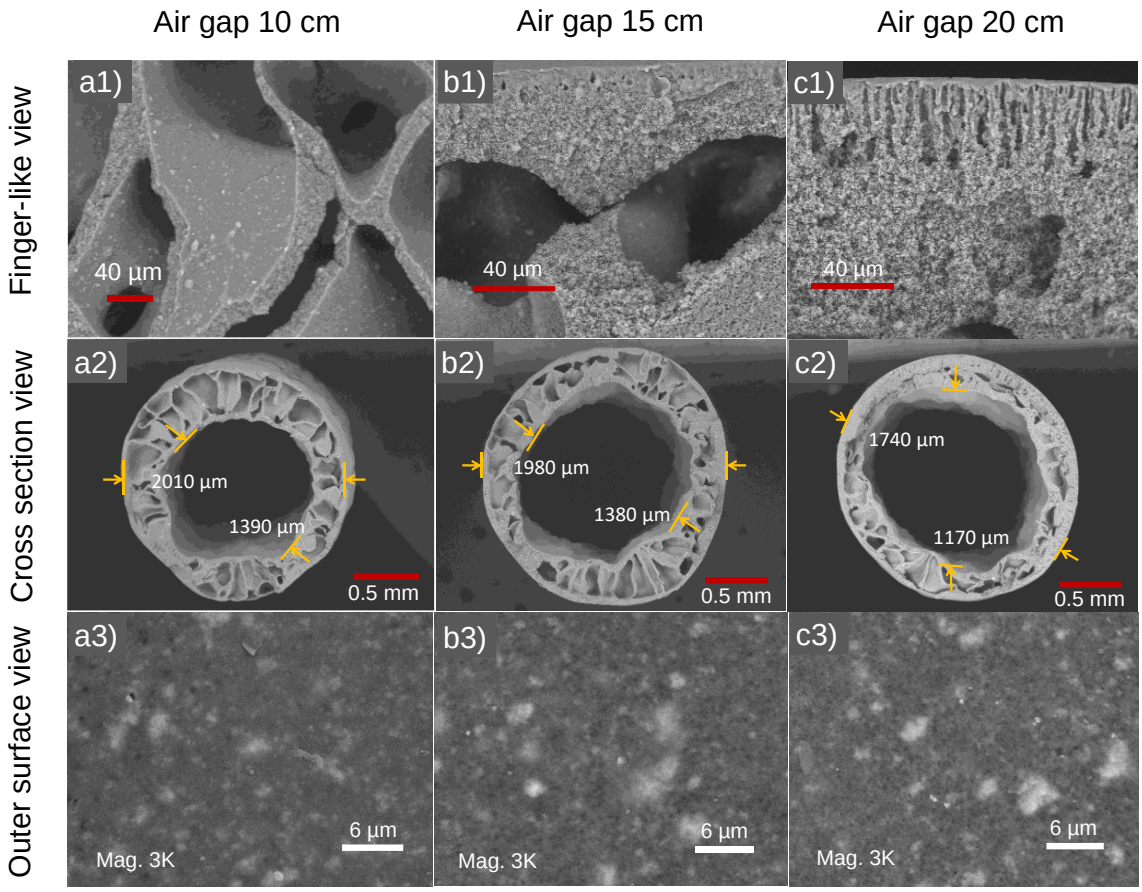

Figure 3. SEM images of the cross-section (a1-c1 and a2-c2) and surface (a3-c3), showing the microstructure and morphology of PVDF-TiO_2 membranes.

The air gap is one of the primary variables that influence membrane morphology. The gravity forces of the falling film during the spinning process imposed elongational stress on the hollow fiber membrane in the air gap region during the dry-wet spinning process. As the air gap increased, the membrane tended to elongate, followed by a decrease in diameter and fiber thickness. **Figure 3 (a1-c1)** shows the outer diameter (OD) of the membranes were 2010, 1980, and 1740 µm for air gaps of 10, 15, and 20 cm, respectively. Meanwhile, the inner diameter (ID) of the membranes were 1390, 1380, and 1170 µm for the air gaps of 10, 15, and 20 cm, respectively. Each membrane with variations of air gap has a thickness of 620, 600, and 570 nm. Similar results were also found by Okubo *et al*. (1991) and Abidin *et al*. (2020).

The shortest air gap distance produced the thickest membrane with the largest OD and the smallest ID attributed to the effect of die swell in the membrane polymers. Die swell occurred because the material had elasticity (i.e. polymers), and experienced extrusion on the die channel when flew out through the spinneret. After that, the polymers instantly swell because of their viscoelasticity properties (Peng *et al*., 2008). Such findings prove that the effect of gravity force on air gap impacts polymer deformation during the dry-wet spinning process (Chung *et al*., 1999).

The polymer has strong intermolecular interactions. At a certain level, it only deformed and did not break the interactions between molecules under stress. This deformation caused the molecules in the polymer to find a new balance to maintain the intermolecular interactions (Khayet, 2003). Therefore, it is possible to a form hollow fiber membrane with a smaller diameter and thickness by increasing the air gap.

DOI: https://doi.org/10.17509/ijost.v8i3.63433
p- ISSN 2528-1410 e- ISSN 2527-8045

The air gap does not only affect the dimensions of the membrane but also affects the structure formed in the membrane matrix. Smaller air gaps tend to form finger-like macro voids. This kind of macro void is highly undesirable because it imparts a low mechanical strength in the resultant membrane. As the air gap increases, the macro void changes from finger-like to sponge-like. This type is more desirable and has better mechanical properties. Sponge-like structures have a smaller void volume than finger-like structures (Gao, 2017). The membrane structure was denser in the more significant air gap than the smaller air gap as illustrated in **Figure 3**. In summary, the membrane morphology was affected by two main mechanisms; a) the orientation of the molecules on the membrane and elongation stress due to gravity effect on the air gap, and b) shear stress and elongation stress in the spinneret (Khayet, 2003).

The hydrophilicity test was performed by the contact angle analysis. The contact angle analysis quantifies the interfacial interaction between solids and liquids to determine the hydrophilicity of the membranes. The membrane can be indicated as hydrophilic when the liquid spreads well on the membrane surface with a contact angle value below 90° (Law, 2014).

The contact angle value (θ) of the PVDF-TiO_2 membrane was 62° as shown in **Figure 4**. PVDF is a polymer-based material frequently used in membrane fabrication. It has hydrophobic properties with a contact angle value of 90° (Zou *et al*., 2020). Meanwhile, pure TiO_2 has excellent hydrophilic properties, outstanding chemical stability, and potential as an anti-fouling agent (Hong *et al*., 2017). Blending TiO_2 particles into the polymer-based membrane matrix imparted hydrophilicity properties into the resultant material (Huang *et al*., 2017; Méricq *et al*., 2015; Qin *et al*., 2015). Such changes were attributed to TiO_2 properties, which consisted of highly oxygenated hydrophilic functional groups Hong *et al*., (2017) that had a higher affinity towards water than the pristine PVDF membrane (Damodar *et al*., 2009).

The FTIR spectra of the PVDF-TiO_2 membrane are shown in **Figure 5a**. A step-by-step analysis of the chemical bonds identified from the FTIR spectra is presented as follows. FTIR analysis is a qualitative method to determine the functional groups composed within the membrane matrix (Sakarkar *et al*., 2021). The fingerprint-like peaks appeared at the wavelength range from 700 to 1500 cm^{-1} and corresponded to the characteristic of PVDF functional groups, consisting of α, β, and γ crystalline phases. The vibration bond found at peaks 763-766 (Medeiros *et al*., 2018; Mun *et al*., 2018), 795, 854, and 975 cm^{-1} is the characteristic peak of α crystalline phase (Cai *et al*., 2017).

The characteristic peak for the β crystalline phase was observed at 1275 cm^{-1} (Cai *et al*., 2017; Medeiros *et al*., 2018). The γ crystalline phase characteristic peak was also found at 1234 cm^{-1}. The peaks in the range of 860 – 900 and 1050 – 1200 cm^{-1} represented the combination of α, β, and γ crystalline phases, which were also reported elsewhere (Benz *et al*., 2002; Cai *et al*., 2017; Kaspar *et al*., 2020; Yoon *et al*., 2008). The absorption bands found at 820 – 860 and 1140 – 1280 cm^{-1} were characteristic of asymmetrical stretching and symmetrical stretching of CF_2, respectively (Sakarkar *et al*., 2021). In addition, the peaks 1403 cm^{-1} and 1640 cm^{-1} were attributed to $–CH_2$ from PVDF and –OH from TiO_2 stretching vibration (Bai *et al*., 2012; Qin *et al*., 2015; Yu *et al*., 2003). Furthermore, the absorption from 800 to 900 cm^{-1} represented a mixed band of $–CH_2$ rocking and $–CF_2$ asymmetric stretching in α, β, γ phases or a combination of the three phases (Cai *et al*., 2017).

Figure 5(b) represents the XRD spectra of the PVDF-TiO_2 membranes in uncalcined and calcined conditions. Step-by-step analysis of the membrane crystallinity identified from the XRD spectra is detailed as follows.

DOI: https://doi.org/10.17509/ijost.v8i3.63433
p- ISSN 2528-1410 e- ISSN 2527-8045

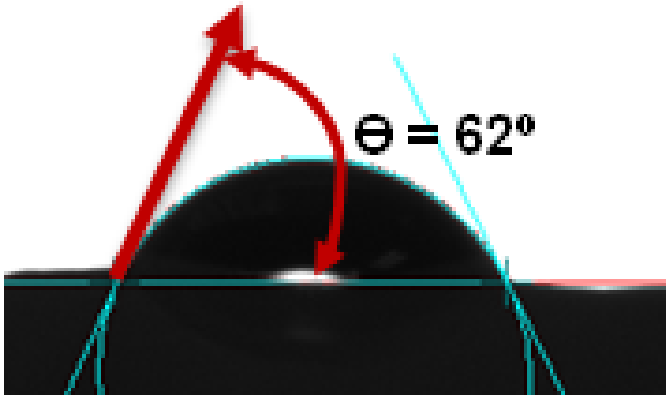

Figure 4. Typical contact angle image of PVDF-TiO_2 hollow fiber membrane.

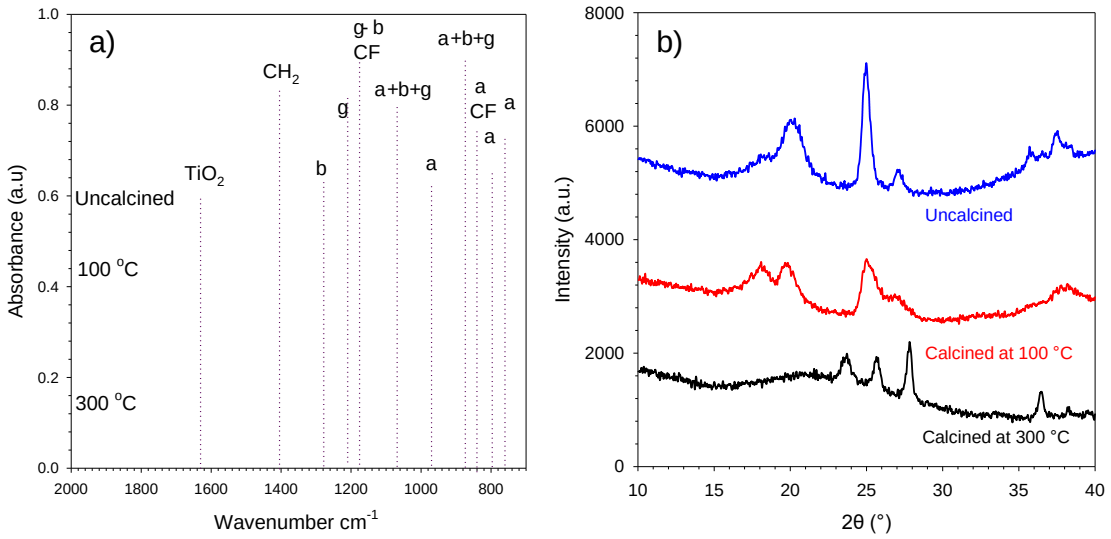

Figure 5. a) FTIR spectra and b) XRD spectra of the PVDF-TiO_2 hollow fiber membrane in various conditions.

The peaks at around 18 and 21° belonged to the PVDF matrix that showed the appearance of α crystalline phase and β crystalline phase, respectively (Cai *et al.*, 2017; Kaspar *et al.*, 2020). Meanwhile, the peaks at approximately 25 and 37° represented TiO_2 particles, indicating that TiO_2 retained its crystalline phase within the membrane matrix (Sakarkar *et al.*, 2021).

The XRD analysis confirmed that the β phase dominated the crystal composition of the PVDF-TiO_2 membrane. It was proven by the distinct diffraction peak of β crystalline phase compared to α crystalline phase for the uncalcined and calcined membranes. However, the diffraction peaks of α and β crystalline phases decreased significantly at 300°C. Such changes could be attributed to the decomposition of the polymer materials at a higher temperature (Mun *et al.*, 2018). The diffraction peaks at around 25.5 and 37° indicated the TiO_2 crystal remained in the membrane matrix and did not decompose at higher temperatures (Sakarkar *et al.*, 2021). These findings were in tandem with the FTIR analysis.

3.3. Pervaporation of Wetland Saline Water

The performance of PVDF-TiO_2 membranes spun at different air gaps for desalination of varied feeds of wetland saline water is shown in **Figure 6**. The water fluxes of the PVDF-TiO_2 membrane spun at air gaps 10, 15, and 20 cm were 10.36; 6.48; and 3.81 kg/m^2.h, respectively for pure water permeation. The result demonstrated that

DOI: https://doi.org/10.17509/ijost.v8i3.63433
p- ISSN 2528-1410 e- ISSN 2527-8045

the pure water permeation increased by decreasing the air gap from 20 to 10 cm. It is due to the longer air gap's length that led to the formation of a thinner separation layer, as discussed elsewhere (Yu *et al*., 2009). A similar trend was also observed at different feed water conditions, i.e., brackish, saline wetland, seawater, and brine water (**Figure 6**). For instance, PVDF-TiO_2 spun at a 10 cm air gap recorded the highest permeate flux for brackish water, surpassed that of air gap at 15 and 20 cm by 34.8 and 70%, respectively.

The air gap has a crucial effect on the cross-section morphology and performance of the PVDF-TiO_2 hollow fiber membrane. Increasing air gap resulted in low permeability and high solute rejection (Gao, 2017). It can be well correlated with the morphology of the membrane. As the finger-like pores reduced at longer air gap length, the permeate fluxes decreased (Zakria *et al*., 2021). This is corroborated by the SEM cross-sectional images shown in **Figure 3**c1 which incorporated a denser sponge-like structure consisting of a small amount of finger-like pores within the membrane matrix.

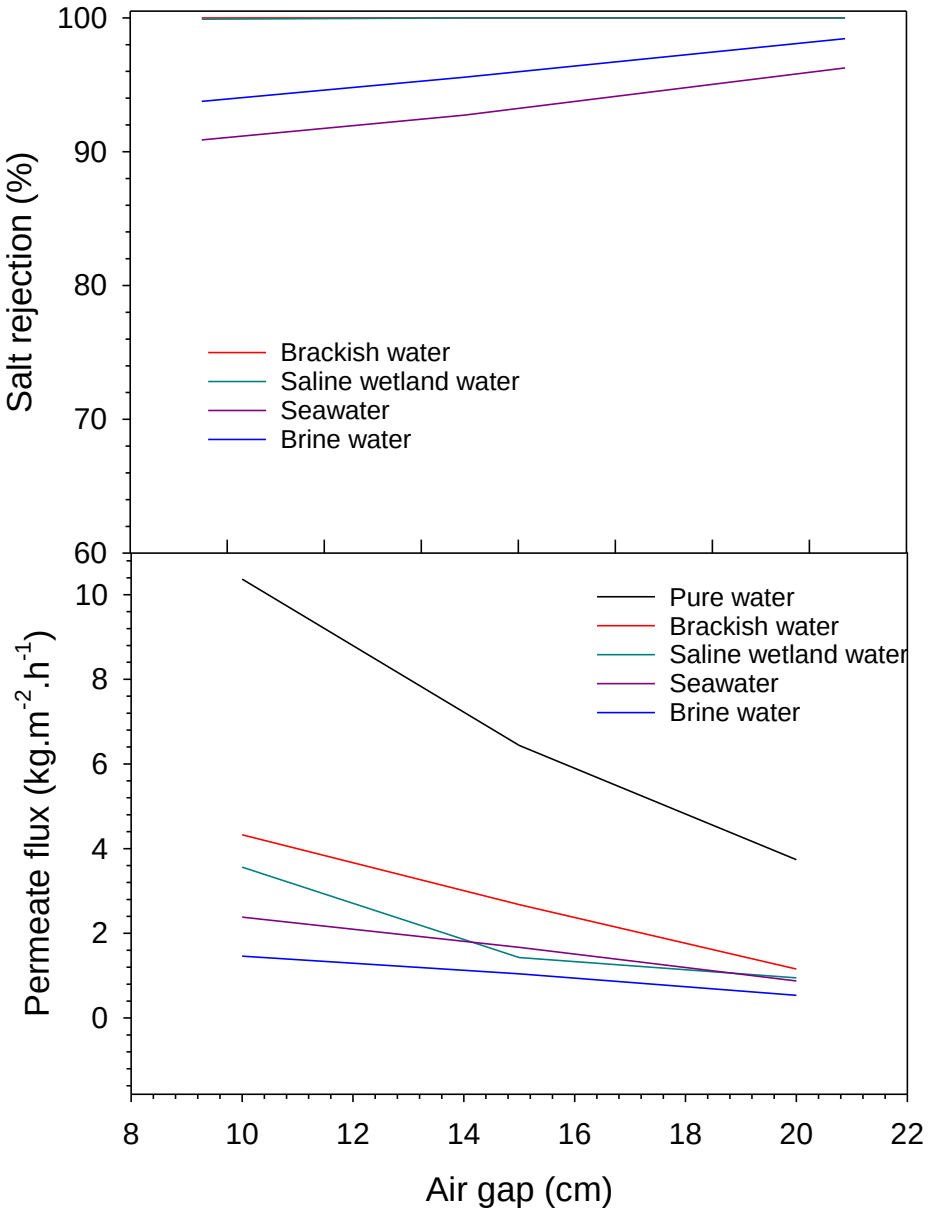

Figure 6. Effect of air gap during the dry-wet spinning on the pervaporation performance of PVDF-TiO_2 hollow fiber membranes treating various feeds.

DOI: https://doi.org/10.17509/ijost.v8i3.63433
p- ISSN 2528-1410 e- ISSN 2527-8045

The permeation performances of PVDF-TiO_2 hollow fiber membrane spun at 10 cm for multiple saline water feed desalination were in the order of brackish > saline wetland > sweater > brine water. Reduction in permeate fluxes as the feed saline concentration increased from 0.3 (brackish) to 5 wt% NaCl (brine) was attributed to the salt concentration polarization effect (Elma *et al.*, 2015). The driving force for salt diffusion increased across the membrane due to the increase in feed salt concentration at the membrane surface (Elma *et al.*, 2013).

Moreover, salt rejections of 90.6-99, 92.6-99.8, and 96-99.7% were recorded for membranes spun at air gaps of 10, 15, and 20 cm in multiple feed water conditions, respectively. As increasing air gap length from 10 to 20 cm, the salt rejection also increased. The air gap length allows the membrane morphology to restrain the NaCl molecule via its thinner and denser finger-like structure (Khayet, 2003). In addition, the longer length of the air gap enables modulation of the distribution of TiO_2 nanoparticles within the outer surface membrane layer, which causes the membrane to become hydrophilicity and improves salt rejection (Yaacob *et al.*, 2020). Salt rejection was generally very high with more than 91% for all air gaps and feed water conditions.

The PVDF-TiO_2 membrane was also tested at various feed temperatures to investigate the pervaporation performance. They were determined by permeability and permselectivity as shown in **Figure 7(a)** and **(b)**. It shows the effect of temperature on the water flux at various feed water conditions at a fixed pervaporation time of 20 minutes. The water flux of wetland saline water was higher than the feed with 3.5 wt% NaCl solution (simulating sea water) but was lower than the feed with 0.3 wt % NaCl solution. The highest water flux of NaCl 0.3 wt%, wetland saline water, and NaCl 3.5 wt% solutions were 15.19, 13.64, and 8.78 kg/m^2.h at 60 °C, respectively. The finding could be attributed to the effect of different salt concentrations in each feed. High salt concentration led to the flux decline caused by concentration polarization (Elma *et al.*, 2012). The pervaporation process of wetland saline water was previously using an interlayer-free-silica-pectin membrane. It was found that the water fluxes of the same wetland saline water (using pectin concentrations of 0.5 and 2.5 wt% as template) were 4.78 and 3.22 kg/m^2.h, respectively. Thus, the pervaporation process using PVDF-TiO_2 hollow fiber membrane had excellent performance because it produced a higher water flux than using an interlayer-free-silica-pectin membranes.

The decline of salt rejection in permeate was observed with the increase in the feed temperature. The decrease of salt rejection followed the order of 60 > 40 > 25°C. Such findings can be well correlated with the condition caused by a random movement of polymer chains under the effect of temperature. The polymer chain movement (expansion) led to the enlargement of membrane pores, which facilitated the diffusion of salt molecules freely through the membrane (Jyoti *et al.*, 2015). The salt rejections for all feed temperatures were higher than 90%, and the highest was 99.9% at 25°C for the wetland saline water. This result is similar to the previous work conducted by other researchers.

Total dissolved solid (TDS) removal and UV_{254} absorbance were measured to determine the membrane's ability to remove the dissolved solids and organic impurities as shown in **Figure 8**. All the TDS removal of wetland saline water at various feed water conditions showed higher than 99.99%. This result indicated that the pervaporation process using PVDF-TiO_2 hollow fiber membrane successfully removed the dissolved solid in wetland saline water. UV_{254} absorbance of the wetland saline water at 25, 40, and 60°C were 98.58, 89.87, and 87.47%, respectively. UV_{254} absorbance decreased

DOI: https://doi.org/10.17509/ijost.v8i3.63433
p- ISSN 2528-1410 e- ISSN 2527-8045

along with the increase in the feed temperature originating from the presence of organic foulant found on the membrane surface. The wetland saline water had a brown color and high NOM constituted of high humic materials (Mahmud & Noor, 2005). The high concentration of polarization of NOM in water contributed to membrane fouling (Goh *et al*., 2018). UV_{254} absorbance was lower than TDS rejection because the wetland saline water contained high humic material which caused the membrane fouling during the pervaporation process, while TDS rejection was not affected by the presence of NOM.

The performance of several types of membranes applied for wetland saline water desalination is summarized in **Table 2**. The developed PVDF-TiO_2 hollow fiber showed decent performance at moderate feed temperature. It was proven by the higher water flux value than previous reportswith the salt rejection of more than 99.5%.

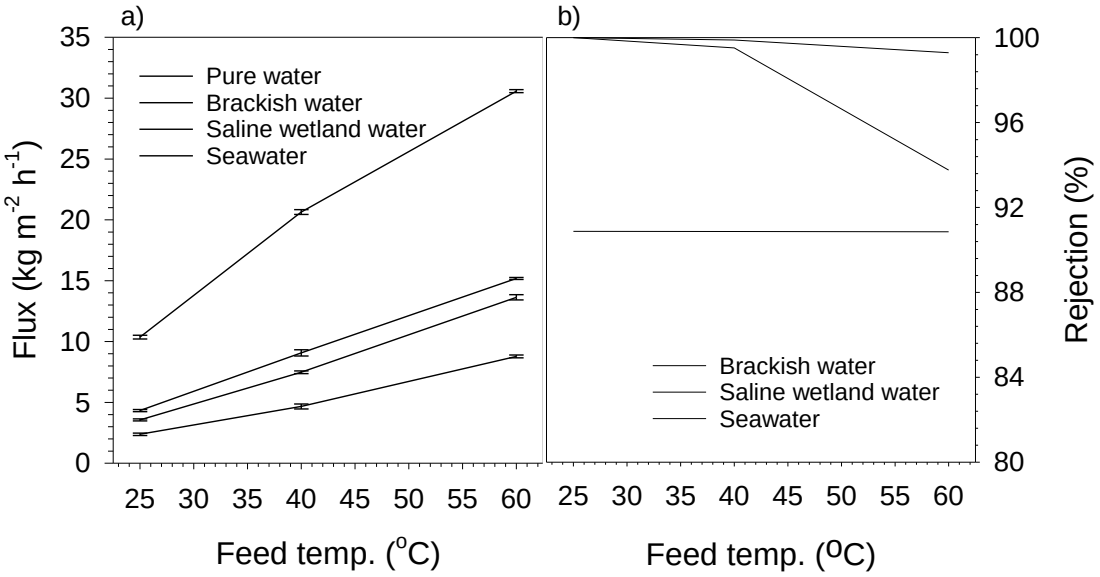

Figure 7. Water flux (a) and salt rejection (b) of PVDF-TiO_2 hollow fiber membrane at various feed temperatures.

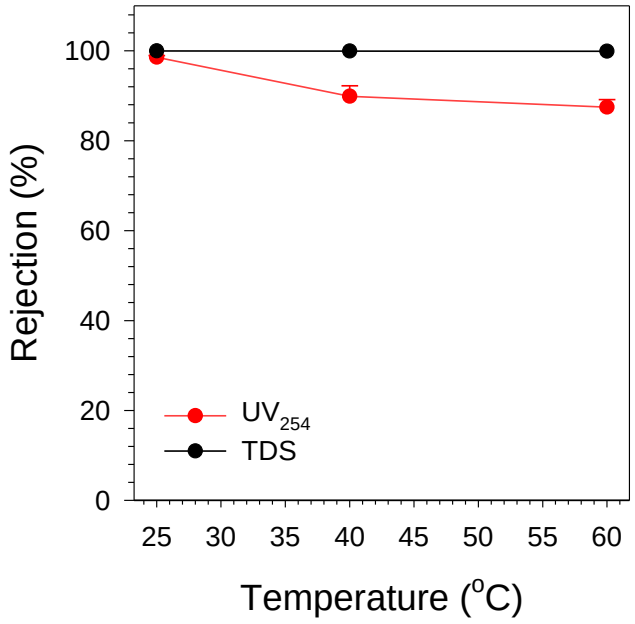

Figure 8. Effect of the feed temperature variations (25°C, 40°C, and 60°C) on TDS removal and UV_{254} absorbance of wetland saline water.

DOI: https://doi.org/10.17509/ijost.v8i3.63433
p- ISSN 2528-1410 e- ISSN 2527-8045

Table 2. Comparison of of several types of membranes used for desalination of wetland saline water.

Type of membranes	Feed Temperature (°C)	Feed Types	Water Flux (kg/m^2.h)	Salt Rejection (%)	References
PVDF-TiO_2 hollow fiber membrane	40	Wetland saline water	7.48	>99.5	This research
CTA/Al_2O_3 hollow fiber membrane	70	Wetland saline water	6.7	99.8	(Prihatiningtyas *et al*., 2020)
Silica-Pectin	25	Wetland saline water	4.48	99.9	(Rahma, Elma, Mahmud, Irawan, *et al*., 2019)
Coagulation (Silica-Pectin)	25	Wetland saline water	5.4	99.9	(Rahma, Elma, Mahmud, Irawan *et al*., 2019)
Alumina hollow fiber membrane	80	Wetland saline water	42.9	99.5	(Fang *et al*., 2012)

4. CONCLUSION

PVDF-TiO_2 hollow fiber membrane was successfully prepared and characterized. The results show that membrane morphology (OD, ID, and thickness) decreased with the increasing the air gap. The resultant membrane imparted hydrophilic properties as TiO_2 particles blended well within the membrane matrix as visually observed from the SEM images. The presence of TiO_2 was confirmed through the observed diffraction peaks at 25.5 and 37°. The highest water flux and salt rejection were observed at 7.48 kg/m^2.h and > 99.5 wt% at 40°C with a decent percentage of TDS and NOMs removal. Overall, it can be concluded that the PVDF-TiO_2 hollow fiber membrane showed the potential to treat wetland saline water via the pervaporation process.

5. ACKNOWLEDGMENT

Muthia thanks to the Advanced Membrane Technology Research Centre (AMTEC), University Teknologi Malaysia (UTM) and Materials and Membranes Research Group (M^{2}ReG), Lambung Mangkurat University for the facilities. Also, thanks to the oil palm research grant 2022 [PRJ-371/DPKS/2022] and the Oil Palm Plantation Fund Management Agency Republic of Indonesia for the financial support. Muthia Elma also thanks to Applied Research Universities Grant 2023 [026/E5/PG.02.00.PL/2023] Thesis Grant [130/E5/PG.02.00.PL/2023 the Ministry of Research and Technology/National Research and Innovation Agency, the Ministry of Education and Culture of the Republic of Indonesia.

6. AUTHORS' NOTE

The authors declare that there is no conflict of interest regarding the publication of this article. The authors confirmed that the paper was free of plagiarism.

DOI: https://doi.org/10.17509/ijost.v8i3.63433
p- ISSN 2528-1410 e- ISSN 2527-8045

7. REFERENCES

Abidin, M. N. Z., Goh, P. S., Said, N., Ismail, A. F., Othman, M. H. D., Abdullah, M. S., Mansur, S. (2020). Polysulfone/amino-silanized poly(methyl methacrylate) dual layer hollow fiber membrane for uremic toxin separation. *Separation and Purification Technology, 236*, 116216.

Bai, H., Wang, X., Zhou, Y., and Zhang, L. (2012). Preparation and characterization of poly (Vinylidene fluoride) composite membranes blended with nano-crystalline cellulose. *Progress in Natural Science: Materials International, 22*, 250–257.

Benz, M., Euler, W. B., and Gregory, O. J. (2002). The role of solution phase water on the deposition of thin films of poly (vinylidene fluoride). *Macromolecules, 35*(7), 2682-2688.

Cai, X., Lei, T., Sun, D., and Lin, L. (2017). A critical analysis of the α, β and γ phases in poly(vinylidene fluoride) using FTIR. *RSC Advances, 7*(25), 15382-15389.

Chung, T.-S., Xu, Z.-L., and Lin, W. (1999). Fundamental understanding of the effect of air-gap distance on the fabrication of hollow fiber membranes. *Journal of Applied Polymer Science, 72*(3), 379-395.

Damodar, R. A., You, S.-J., and Chou, H.-H. (2009). Study the self cleaning, antibacterial and photocatalytic properties of TiO2 entrapped PVDF membranes. *Journal of Hazardous Materials, 172*(2), 1321-1328.

Dayarathne, H. N. P., Angove, M. J., Aryal, R., Abuel-Naga, H., and Mainali, B. (2021). Removal of natural organic matter from source water: Review on coagulants, dual coagulation, alternative coagulants, and mechanisms. *Journal of Water Process Engineering, 40*, 101820.

Deshmukh, S. P., and Li, K. (1998). Effect of ethanol composition in water coagulation bath on morphology of PVDF hollow fibre membranes. *Journal of Membrane Science, 150*(1), 75-85.

Dzinun, H., Othman, M. H. D., Ismail, A., Puteh, M. H., Rahman, M. A., and Jaafar, J. (2016). Photocatalytic degradation of nonylphenol using co-extruded dual-layer hollow fibre membranes incorporated with a different ratio of TiO2/PVDF. *Reactive and Functional Polymers, 99*, 80-87.

Elma, M., Bilad, M. R., Pratiwi, A. E., Rahma, A., Asyyaifi, Z. L., Hairullah, H., Lestari, R. A. (2022). Long-term performance and stability of interlayer-free mesoporous silica membranes for wetland saline water pervaporation. *Polymers, 14*(5), 895.

Elma, M., Ghani, R. A., Rahma, A., Alyanti, A. D., and Dony, N. (2022). Banana peels pectin templated silica ultrafiltration membrane in disk plate configuration applied for wetland water treatment. *Journal of Advanced Research in Fluid Mechanics and Thermal Sciences, 100*(1), 77-88.

Elma, M., Mujiyanti, D. R., Ismail, N. M., Bilad, M. R., Rahma, A., Rahman, S. K., Rampun, E. L. A. (2020). Development of hybrid and templated silica-p123 membranes for brackish water desalination. *Polymers, 12*(11), 2644.

DOI: https://doi.org/10.17509/ijost.v8i3.63433
p- ISSN 2528-1410 e- ISSN 2527-8045

Elma, M., Pratiwi, A. E., Rahma, A., Rampun, E. L. A., Mahmud, M., Abdi, C., Bilad, M. R. (2022). Combination of coagulation, adsorption, and ultrafiltration processes for organic matter removal from peat water. *Sustainability, 14*(1), 370.

Elma, M., Rahma, A., Kusumawati, U., Pratama, R. K., and Alyanti, A. D. (2022). Single vs multichannel silica-pectin ultrafiltration membranes for treatment of natural peat water. *Journal of Advanced Research in Fluid Mechanics and Thermal Sciences, 100*(2), 33-46.

Elma, M., Rampun, E. L. A., Rahma, A., Assyaifi, Z. L., Sumardi, A., Lestari, A. E., Darmawan, A. (2020). Carbon templated strategies of mesoporous silica applied for water desalination: A review. *Journal of Water Process Engineering, 38*, 101520.

Elma, M., Septyaningrum, L., Rahmawati, and Rahma, A. (2023). Vacuum versus air calcination of modified TEOS-MTES based membrane for seawater desalination. *AIP Conference Proceedings, 2711*(1), 050002.

Elma, M., Wang, D. K., Yacou, C., and Costa, J. C. D. d. (2015). Interlayer-free P123 carbonised template silica membranes for desalination with reduced salt concentration polarisation. *Journal of Membrane Science, 475*, 376-383.

Elma, M., Yacou, C., Costa, J. C. D. d., and Wang, D. K. (2013). Performance and long term stability of mesoporous silica membranes for desalination. *Membranes, 3*, 136-150.

Elma, M., Yacou, C., Wang, D. K., Smart, S., and Diniz da Costa, J. C. (2012). Microporous silica based membranes for desalination, *Water, 4*(3), 629.

Fan, H., and Peng, Y. (2012). Application of PVDF membranes in desalination and comparison of the VMD and DCMD processes. *Chemical Engineering Science, 79*, 94-102.

Fang, H., Gao, J., Wang, H., and Chen, C. (2012). Hydrophobic porous alumina hollow fiber for water desalination via membrane distillation process. *Journal of Membrane Science, 403*, 41-46.

Gao, Y. (2017). Correlated Effect of Air Gap and PVP Concentration on the Structure and Performance of PVDF Ultrafiltration Hollow Fiber Membrane. *Journal of Membrane Science and Research, 3*(2), 78-83.

Goh, P., Lau, W. J., Othman, M. H., and Ismail, A. (2018). Membrane fouling in desalination and its mitigation strategies. *Desalination, 425*, 130-155.

Hong, X., Zhou, Y., Ye, Z., Zhuang, H., Liu, W., Hui, K. S., Qiu, X. (2017). Enhanced hydrophilicity and antibacterial activity of PVDF ultrafiltration membrane using Ag3PO4/TiO2 nanocomposite against E. coli. *Desalination and Water Treatment, 75*, 26-33.

Huang, L., Jing, S., Zhuo, O., Meng, X., and Wang, X. (2017). Surface hydrophilicity and antifungal properties of TiO_2 films coated on a Co-Cr substrate. *BioMed Research International, 2017*, 2054723.

Jyoti, G., Keshav, A., and Anandkumar, J. (2015). Review on pervaporation: Theory, membrane performance, and application to intensification of esterification reaction. *Journal of Engineering, 2015*, 927068.

Kamaludin, R., Mohamad Puad, A. S., Othman, M. H. D., Kadir, S. H. S. A., and Harun, Z. (2019). Incorporation of N-doped TiO2 into dual layer hollow fiber (DLHF) membrane for visible light-driven photocatalytic removal of reactive black 5. *Polymer Testing, 78*, 105939.

DOI: https://doi.org/10.17509/ijost.v8i3.63433
p- ISSN 2528-1410 e- ISSN 2527-8045

Kaspar, P., Sobola, D., Částková, K., Knápek, A., Burda, D., Orudzhev, F., Hadaš, Z. (2020). Characterization of polyvinylidene fluoride (PVDF) electrospun fibers doped by carbon flakes. *Polymers, 12*(12), 2766.

Khayet, M. (2003). The effects of air gap length on the internal and external morphology of hollow fiber membranes. *Chemical Engineering Science, 58*(14), 3091-3104.

Khulbe, K. C., Feng, C. Y., Matsuura, T., Mosqueada-Jimenaez, D. C., Rafat, M., Kingston, D., Khayet, M. (2007). Characterization of surface-modified hollow fiber polyethersulfone membranes prepared at different air gaps. *Journal of Applied Polymer Science, 104*(2), 710-721.

Kingsbury, B. F. K., and Li, K. (2009). A morphological study of ceramic hollow fibre membranes. *Journal of Membrane Science, 328*(1), 134-140.

Law, K.-Y. (2014). Definitions for hydrophilicity, hydrophobicity, and superhydrophobicity: Getting the basics right. *The Journal of Physical Chemistry Letters, 5*(4), 686-688.

Li, L., Hou, J., Ye, Y., Mansouri, J., and Chen, V. (2017). Composite PVA/PVDF pervaporation membrane for concentrated brine desalination: Salt rejection, membrane fouling and defect control. *Desalination, 422*, 49-58.

Li, X., Chen, Y., Hu, X., Zhang, Y., and Hu, L. (2014). Desalination of dye solution utilizing PVA/PVDF hollow fiber composite membrane modified with TiO2 nanoparticles. *Journal of Membrane Science, 471*, 118-129.

Mahmud, Elma, M., Rampun, E. L. A., Rahma, A., Pratiwi, A. E., Abdi, C., and Rosadi, R. (2020). Effect of two stages adsorption as pre-treatment of natural organic matter removal in ultrafiltration process for peat water treatment. *Materials Science Forum, 988*, 114-121.

Mahmud, M., and Noor, R. (2005). Kinetika fouling membran ultrafiltrasi (UF) pada pengolahan air berwarna: Pengaruh interval dan lamanya pencucian balik (backwashing) membran. *Info-Teknik, 6*(1), 62-69.

Mat Nawi, N. I., Mohd Lazis, A., Rahma, A., Elma, M., Bilad, M. R., Md Nordin, N. A. H., Yusof, N. (2022). A rotary spacer system for energy-efficient membrane fouling control in oil/water emulsion filtration. *Membranes, 12*(6), 554.

Maulida, N. A., Fitriah, S. H., Aliah, A., Rampun, E. L. A., and Elma, M. (2023). Preparation and performance of interlayer-free organosilica membranes on zirconia support. *AIP Conference Proceedings, 2667*(1), 040011.

Medeiros, K. A. R., Rangel, E. Q., Sant'Anna, A. R., Louzada, D. R., Barbosa, C. R. H., and d'Almeida, J. R. M. (2018). Evaluation of the electromechanical behavior of polyvinylidene fluoride used as a component of risers in the offshore oil industry. *Oil and Gas Science and Technology - Revue d'IFP Energies Nouvelles, 73*, 48.

Méricq, J. P., Mendret, J., Brosillon, S., and Faur, C. (2015). High performance PVDF-TiO2 membranes for water treatment. *Chemical Engineering Science, 123*, 283-291.

Mun, J., Park, H. M., Koh, E., and Lee, Y. T. (2018). Enhancement of the crystallinity and surface hydrophilicity of a PVDF hollow fiber membrane on simultaneous stretching and coating method. *Journal of Industrial and Engineering Chemistry, 65*, 112-119.

DOI: https://doi.org/10.17509/ijost.v8i3.63433
p- ISSN 2528-1410 e- ISSN 2527-8045

Nawi, N. I. M., Arifin, S. N. H. M., Hizam, S. M., Rampun, E. L. A., Bilad, M. R., Elma, M., Jaafar, J. (2020). Chlorella vulgaris broth harvesting via standalone forward osmosis using seawater draw solution. *Bioresource Technology Reports, 9*, 100394.

Okubo, T., Haruta, K., Kusakabe, K., Morooka, S., Anzai, H., and Akiyama, S. (1991). Preparation of a sol-gel derived thin membrane on a porous ceramic hollow fiber by the filtration technique. *Journal of Membrane Science, 59*(1), 73-80.

Parvizian, F., Ansari, F., and Bandehali, S. (2020). Oleic acid-functionalized TiO2 nanoparticles for fabrication of PES-based nanofiltration membranes. *Chemical Engineering Research and Design*, *156*, 433-441.

Peng, N., Chung, T.-S., and Wang, K. Y. (2008). Macrovoid evolution and critical factors to form macrovoid-free hollow fiber membranes. *Journal of Membrane Science, 318*(1), 363-372.

Pratiwi, E. N., Elma, M., Mahmud, M., Basir, B., Rezki, M. R., Oktaviana, E. N. R., Rahma, A. (2023). Novel carbon templated silica membrane prepared from Nypa fruticans leaf for seawater desalination. *AIP Conference Proceedings, 2682*(1), 030006.

Prihatiningtyas, I., Gebreslase, G. A., and Van der Bruggen, B. (2020). Incorporation of Al2O3 into cellulose triacetate membranes to enhance the performance of pervaporation for desalination of hypersaline solutions. *Desalination, 474*, 114198.

Qin, A., Li, X., Zhao, X., Liu, D., and He, C. (2015). Engineering a highly hydrophilic PVDF membrane via binding TiO2 nanoparticles and a PVA layer onto a membrane surface. *ACS Applied Materials and Interfaces, 7*(16), 8427-8436.

Rahma, A., Elma, M., Aliah, Kusumawati, U., and Dony, N. (2022). Novel multi-channel coated silica based membranes applied for peat water ultrafiltration. *Journal of Advanced Research in Fluid Mechanics and Thermal Sciences, 100*(3), 133-145.

Rahma, A., Elma, M., Mahmud, M., Irawan, C., Pratiwi, A. E., and Rampun, E. L. A. (2019). Penyisihan bahan organik alami pada desalinasi air rawa asin menggunakan proses koagulasi-Pervaporasi. *Jurnal Kimia Sains dan Aplikasi*, *22*(3), 85-92.

Rahma, A., Elma, M., Pratiwi, A. E., and Rampun, E. L. (2020). Performance of interlayer-free pectin template silica membranes for brackish water desalination. *Membrane Technology, 2020*(6), 7-11.

Rahma, A., Elma, M., Rampun, E. L. A., Pratiwi, A. E., Rakhman, A., and Fitriani. (2020). Rapid thermal processing and long term stability of interlayer-free silica-P123 membranes for wetland saline water desalination. *Advanced Research in Fluid Mechanics and Thermal Sciences, 71*(2), 1-9.

Rahma, A., Elma, M., Roil Bilad, M., Isnasyauqiah, Rahman Wahid, A., Sirajul Huda, M., and Resa Lamandau, D. (2023). Novel spent bleaching earth industrial waste as low-cost ceramic membranes material: elaboration and characterization. *Materials Today: Proceedings*, *87*(2), 136-140.

Rampun, E. L. A., Elma, M., Rahma, A., and E.Pratiwi, A. (2019). Interlayer-free silica–pectin membrane for sea-water desalination. *Membrane Technology, 2019*(12), 5-9.

DOI: https://doi.org/10.17509/ijost.v8i3.63433
p- ISSN 2528-1410 e- ISSN 2527-8045

Rampun, E. L. A., Elma, M., Syauqiah, I., Putra, M. D., Rahma, A., and Pratiwi, A. E. (2019). Interlayer-free silica pectin membrane for wetland saline water via pervaporation. *Jurnal Kimia Sains dan Aplikasi, 22*(3), 99-104.

Sakarkar, S., Muthukumaran, S., and Jegatheesan, V. (2020). Polyvinylidene fluoride and titanium dioxide ultrafiltration photocatalytic membrane: Fabrication, morphology, and its application in textile wastewater treatment. *Journal of Environmental Engineering, 146*(7), 04020053.

Sakarkar, S., Muthukumaran, S., and Jegatheesan, V. (2021). Tailoring the effects of titanium dioxide (TiO2) and polyvinyl alcohol (PVA) in the separation and antifouling performance of thin-film composite polyvinylidene fluoride (PVDF) membrane. *Membranes, 11*(4), 241.

Sari, D. P., Elma, M., Mahmud, M., Basir, B., Rezki, M. R., Rahmawati, R., Rahma, A. (2023). Fabrication of organo-silica thin film for water desalination from dual silicate precursor (tetraethylorthosilicate and methyltriethoxysilane). *AIP Conference Proceedings, 2682*(1), 030007.

Satria Anugerah, S., Elma, M., Isna, S., Dwi Resa, L., Siti, F., and Aulia, R. (2022). Energy from salinity gradient of wetland saline water using reverse electrodialysis membrane. *Journal of Advanced Research in Fluid Mechanics and Thermal Sciences, 101*(2), 46-59.

Shi, H., Liu, F., and Xue, L. (2013). Fabrication and characterization of antibacterial PVDF hollow fibre membrane by doping Ag-loaded zeolites. *Journal of Membrane Science, 437*, 205-215.

Sun, J., Qian, X., Wang, Z., Zeng, F., Bai, H., and Li, N. (2020). Tailoring the microstructure of poly (vinyl alcohol)-intercalated graphene oxide membranes for enhanced desalination performance of high-salinity water by pervaporation. *Journal of Membrane Science*, *599*, 117838.

Tan, X., and Rodrigue, D. (2019). A review on porous polymeric membrane preparation part i: production techniques with polysulfone and poly (Vinylidene Fluoride). *Polymers, 11*(7), 1160.

Wang, D. K., Elma, M., Motuzas, J., Hou, W.-C., Schmeda-Lopez, D. R., Zhang, T., and Zhang, X. (2016). Physicochemical and photocatalytic properties of carbonaceous char and titania composite hollow fibers for wastewater treatment. *Carbon, 109*, 182-191.

Yaacob, N., Goh, P. S., Ismail, A. F., Mohd Nazri, N. A., Ng, B. C., Zainal Abidin, M. N., and Yogarathinam, L. T. (2020). ZrO2-TiO2 incorporated PVDF dual-layer hollow fiber membrane for oily wastewater treatment: Effect of air gap. *Membranes, 10*(6), 124.

Yoon, S., Prabu, A. A., Kim, K. J., and Park, C. (2008). Metal salt-induced ferroelectric crystalline phase in poly(vinylidene fluoride) films. *Macromolecular Rapid Communications, 29*(15), 1316-1321.

Yu, J.-G., Yu, H.-G., Cheng, B., Zhao, X.-J., Yu, J. C., and Ho, W.-K. (2003). The effect of calcination temperature on the surface microstructure and photocatalytic activity of tio2 thin films prepared by liquid phase deposition. *The Journal of Physical Chemistry B, 107*(50), 13871-13879.

DOI: https://doi.org/10.17509/ijost.v8i3.63433
p- ISSN 2528-1410 e- ISSN 2527-8045

Yu, L.-Y., Shen, H.-M., and Xu, Z.-L. (2009). PVDF–TiO2 composite hollow fiber ultrafiltration membranes prepared by TiO2 sol–gel method and blending method. *Journal of Applied Polymer Science, 113*(3), 1763-1772.

Zou, L., Gusnawan, P., Zhang, G., and Yu, J. (2020). Study of the effective thickness of the water-intrudable hydrophilic layer in dual-layer hydrophilic-hydrophobic hollow fiber membranes for direct contact membrane distillation. *Journal of Membrane Science, 615*, 118552.

DOI: https://doi.org/10.17509/ijost.v8i3.63433
p- ISSN 2528-1410 e- ISSN 2527-8045